JB
Journals.ASM.org

Unique Helicase Determinants in the Essential Conjugative TraI Factor from *Salmonella enterica* Serovar Typhimurium Plasmid pCU1

Krystle J. McLaughlin,[a] Rebekah P. Nash,[a] Mathew R. Redinbo[a,b]

Department of Chemistry[a] and Departments of Biochemistry and Microbiology,[b] University of North Carolina at Chapel Hill, Chapel Hill, North Carolina, USA

The widespread development of multidrug-resistant bacteria is a major health emergency. Conjugative DNA plasmids, which harbor a wide range of antibiotic resistance genes, also encode the protein factors necessary to orchestrate the propagation of plasmid DNA between bacterial cells through conjugative transfer. Successful conjugative DNA transfer depends on key catalytic components to nick one strand of the duplex DNA plasmid and separate the DNA strands while cell-to-cell transfer occurs. The TraI protein from the conjugative *Salmonella* plasmid pCU1 fulfills these key catalytic roles, as it contains both single-stranded DNA-nicking relaxase and ATP-dependent helicase domains within a single, 1,078-residue polypeptide. In this work, we unraveled the helicase determinants of *Salmonella* pCU1 TraI through DNA binding, ATPase, and DNA strand separation assays. TraI binds DNA substrates with high affinity in a manner influenced by nucleic acid length and the presence of a DNA hairpin structure adjacent to the nick site. TraI selectively hydrolyzes ATP, and mutations in conserved helicase motifs eliminate ATPase activity. Surprisingly, the absence of a relatively short (144-residue) domain at the extreme C terminus of the protein severely diminishes ATP-dependent strand separation. Collectively, these data define the helicase motifs of the conjugative factor TraI from *Salmonella* pCU1 and reveal a previously uncharacterized C-terminal functional domain that uncouples ATP hydrolysis from strand separation activity.

Helicases are molecular motors that drive the separation of duplex nucleic acid strands through the coupling of ATP hydrolysis to unwinding (1–3). As a result, helicases are key players in a wide variety of DNA and RNA metabolic processes, such as recombination, chromatin remodeling, and DNA transport (4–6). Most recently, helicases have emerged as potential therapeutic targets for diseases ranging from cancer to Gram-positive bacterial infections (7–18). Classified into six superfamilies, superfamily 1 and 2 (SF1 and SF2) helicases are the most similar, sharing up to seven conserved sequence motifs and core RecA-like folds (1–3). Furthermore, SF1 helicases comprise the largest class and can be further subdivided into SF1A and SF1B, based on the direction of helicase translocation along the strand; SF1A helicases progress 3′ to 5′ and SF1B 5′ to 3′ (3). Despite their importance, SF1B helicases are still poorly characterized in comparison to SF1A and SF2 helicases, though some recent studies have expanded our knowledge (19–21). SF1B helicases are critical to a diverse range of processes, including DNA repair by human DNA helicase B (22), telomere regulation by Pif1 (23), and conjugative plasmid transfer by F TraI (24).

Conjugative plasmid transfer (CPT) mediates the propagation of antibiotic resistance genes and virulence factors within commensal and pathogenic bacteria (25–27) and relies on the helicase domain of a bifunctional protein to facilitate plasmid DNA transfer (24, 28–30). Early work characterizing the general mechanism of CPT was accomplished through the study of the F (fertility) plasmid system, a member of the MOB_F family of conjugative plasmids (31–35). During CPT, a donor bacterium transfers one strand of the double-stranded conjugative DNA plasmid to a neighboring recipient via direct cell-cell contact (29, 36). Conjugative plasmids encode nearly all of the proteins found within the relaxosome, a multiprotein complex indispensable for sequence-specific transfer of the plasmid (37). DNA strand transfer is initiated by a relaxosome component, the relaxase, through a site- and strand-specific DNA nick at the plasmid origin of transfer (*oriT*). Once nicked, a helicase unwinds the duplex DNA plasmid and one strand is transferred through a pore connecting the neighboring cells. In many conjugative systems, the relaxase is found at the N terminus of a multifunctional transfer-initiation protein with a helicase or primase located C terminal to the relaxase (29, 35, 37).

Bifunctional enzymes TraI (1,756 residues) and TrwC (966 residues), from F plasmid and resistance plasmid R388, respectively, harbor an N-terminal relaxase and a C-terminal helicase (38, 39). In both cases, the C-terminal helicase belongs to the SF1B family. Structures of the MOB_F N-terminal relaxases from F TraI and R388 TrwC have been determined (40, 41), and their enzymatic nicking activity has been thoroughly investigated (42–47). Although DNA binding of the F TraI C-terminal helicase has recently been investigated (30, 48), much less is known about the structure and mechanism of these C-terminal helicase domains relative to the N-terminal relaxase domains. Studies of F TraI and R388 TrwC demonstrate, however, that both enzymatic activities of the relaxase and helicase are required for CPT (24, 38, 44). Furthermore, more distantly related relaxases with C-terminal domains lacking in apparent catalytic activity, such as NES from *Staphylococcus aureus* pSK41, have recently been shown to require their relatively large C-terminal domains for conjugative transfer (49).

The relaxase-helicase enzyme TraI, encoded by MOB_F conjugative resistance plasmid pCU1, is responsible for DNA plasmid processing leading to cell-to-cell transfer of the pCU1 plasmid (50–52). The structure and function of the pCU1 TraI N-terminal

Received 24 January 2014 **Accepted** 10 June 2014
Published ahead of print 16 June 2014
Address correspondence to Matthew R. Redinbo, redinbo@unc.edu.
Copyright © 2014, American Society for Microbiology. All Rights Reserved.
doi:10.1128/JB.01496-14

TABLE 1 DNA substrates used in this study

Substrate[a]	Length (nucleotides)	Sequence (5′ to 3′)
DNA binding		
35oriT-hairpin	35	TGTGAT**AGCGTG**ATTTAT**CGCGCT**GCGTTAGGTGT[b]
35-mer-hairpin	35	CTAGCT**CCGAGC**ATAAGA**GCTCGG**ACTACGTGATC[b]
35-mer	35	TGCGTGCGTAGTGTCTATAGCGGAGATCCTGGAGT
19-mer	19	CAGCGAGCGAGCGAACGCG
10-mer	10	AGCGAACGCG
NTPase assays		
23-mer	23	CCTAGATCCCATTGGCCATGAGC
37-mer	37	TCGATCTAGCATCCGGATCTAGGGTAACCGGTACTCG
60-mer	60	GCGATACGTACTGTCGATCCATGTCGATCTAGCATCCGGATCTAGGGTAACCGGTACTCG
Helicase assays		
17-mer	17	CCGGTTACCCTAGATCC
80-mer	80	CTAGGCATTCGACTGCACTAGATCTTGCGATACGTACTGTCGATCCATGTCGATCTAGCA TCCGGATCTAGGGTAACCGG[c]

[a] DNA substrates are all labeled with fluorescein at the 5′ end, with the exception of the 23-mer, 37-mer, 60-mer, and 80-mer substrates.
[b] Bold sequences contain an inverted repeat predicted to form a hairpin structure.
[c] Underline indicates the region that base-pairs with the 17-mer substrate.

relaxase domain have been well studied (53, 54), with only limited data available for its C-terminal helicase. In this work, we establish that the C-terminal domain of pCU1 TraI contains a functional SF1B helicase capable of binding DNA, hydrolyzing ATP and unwinding double-stranded DNA (dsDNA) substrates. We also demonstrate a third functional domain that couples ATP hydrolysis to unwinding activity and is essential for TraI helicase function.

MATERIALS AND METHODS

Expression and purification of pCU1 TraI constructs. The pCU1 TraI constructs used in this study include WT_1078 (residues 1 to 1078; GenBank accession number AAD27542), WT_299 (residues 1 to 299), WT_932 (residues 1 to 932), WT_311-1078 (residues 311 to 1078), WT_483-1078 (residues 483 to 1078), and WT_311-932 (residues 311 to 932) (see Fig. 2). ATPase point mutants were generated by QuikChange site-directed mutagenesis (Stratagene). All TraI constructs were cloned into the pTYB2 vector of the IMPACT system (New England BioLabs) as previously described (4–6, 53).

Cloned constructs were grown in *Escherichia coli* BL21(DE3) cells in 1.5 liters of terrific broth (TB) under ampicillin selection with shaking at 37°C to an optical density of 0.6 to 0.8. Protein expression was induced with isopropyl β-D-1-thiogalactopyranoside (IPTG) added to a final concentration of 0.1 mM, and then the temperature was reduced to 18°C. Protein was overexpressed at 18°C for 16 h, after which the cells were harvested by centrifugation and resuspended in buffer C (500 mM NaCl, 20 mM Tris-HCl [pH 7.5], 10% glycerol, 5 mM EDTA, 0.01% azide). Resuspended cells were stored at −80°C.

All proteins were purified on chitin resin (New England BioLabs) using a batch bind method followed by an extended wash step as described in the manufacturer's protocol. The chitin resin was incubated for 16 h with 50 mM dithiothreitol (DTT) to induce cleavage of the intein and chitin binding domain (CBD) tags and thus release TraI from the intein, CBD, and chitin resin. Eluted TraI constructs were then further purified in an additional size exclusion chromatography step using a HiLoad 16/60 Superdex 200 column (GE Healthcare) preequilibrated with buffer S (100 mM NaCl, 50 to 100 mM Tris-HCl, 0.01% azide) on an ÄKTAxpress fast protein liquid chromatograph (FPLC; GE Healthcare).

Fluorescence anisotropy. The affinity for binding of TraI constructs to several DNA substrates was investigated using fluorescence anisotropy (FA)-based DNA binding assays. Fluorescence measurements were obtained using a PHERAstar fluorescence plate reader (BMG Labtech) at room temperature. High-performance liquid chromatography (HPLC)-purified fluorescein (5′-6-carboxyfluorescein [FAM])-labeled DNA substrates were obtained from Integrated DNA Technologies Inc. (IDT). All DNA substrates were resuspended in buffer R (50 mM NaCl, 10 mM Tris-HCl [pH 7.5], 0.05 mM EDTA, 0.01% azide), heated to 95°C for 10 min, and then allowed to slow cool to room temperature. The DNA nucleotide sequences used are listed in Table 1.

For each assay, the purified protein was initially diluted to 2× the maximum final concentration desired in buffer B (50 mM NaCl, 20 mM Tris-HCl [pH 7.5], 5% glycerol, 5 mM EDTA, 0.01% azide), followed by serial dilutions in buffer B to generate 8 to 16 unique protein concentrations. Fluorescently labeled DNA substrate (0.1 μM) was then combined with an equal volume of each concentration of protein, resulting in a final concentration of 50 nM DNA substrate and 1× protein. Equal volumes of 0.1 μM DNA substrate and buffer B were mixed to generate a no-protein control. The assay was performed in triplicate on a 96- or 384-well black assay plate (Costar). Samples were excited at 490 nm and emission intensities recorded at 520 nm on the PHERAstar fluorescence plate reader in a T format. Depending on the shape of the curve and apparent binding mode observed, the data were fit in Graphpad Prism v6.0 (Graphpad, 2013) using equation 1 (one-site specific binding with Hill slope, Graphpad, 2013) to yield a value for the apparent K_D (equilibrium dissociation constant):

$$f = \frac{(max)x^h}{K_{ap}^h + x^h} \quad (1)$$

where f is average FA signal detected, x is total protein concentration, K_{ap} is apparent K_D, max is average FA signal of sample at a saturating concentration of protein, and h is the Hill coefficient. Alternatively, equation 2 could be used to yield a value for K_D as previously described (7–18, 53):

$$f = min + (max - min)\frac{\left\{(T + X + K) - \left[(-T - X - K)^2 - 4Tx\right]^{\frac{1}{2}}\right\}}{2T} \quad (2)$$

where f is average FA signal detected, T is total DNA concentration (50 nM), x is total protein concentration, K is K_D; min is average FA signal of the no-protein control, and max is average FA signal of sample at a saturating concentration of protein.

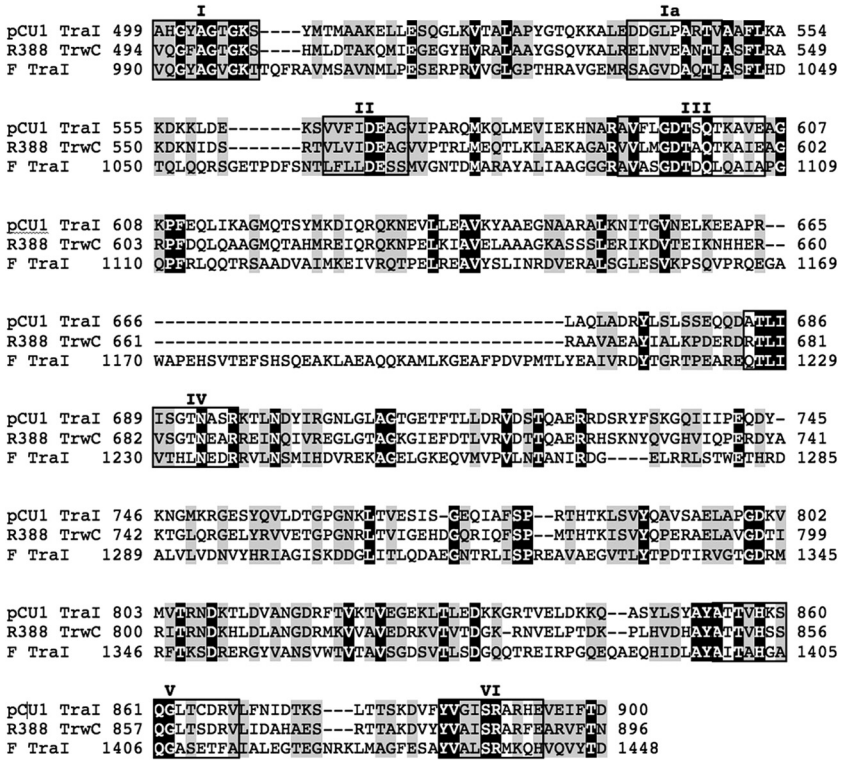

FIG 1 pCU1 TraI helicase sequence alignment. C termini of pCU1 TraI (GenBank accession number AAD27542.1), R388 TrwC (GenBank accession number CAA44853.2), and F TraI (GenBank accession number BAA97974.1) were aligned to show conserved SF1 helicase motifs (boxed). Identical residues are shaded black, and similar residues are shaded gray.

NADH-linked enzyme NTPase assay. NTPase activity of pCU1 TraI was evaluated using a NADH-linked enzyme assay involving pyruvate kinase (PK) and lactate dehydrogenase (LDH), as described by Kiianitsa et al. (55). The drop in absorbance over time was monitored at 350 nm by a PHERAstar fluorescence plate reader (BMG Labtech) and was used to calculate the rate of nucleoside triphosphate (NTP) hydrolysis by pCU1 TraI using equation 3 (1–3, 55):

$$\text{NTPase rate}\left[\text{NTP} \times \text{min}^{-1}\right] = n\frac{dA_{350}}{dt}\left[\frac{\text{OD}}{\text{min}}\right] \times K_{path}^{-1} \times \text{moles}^{-1}\ \text{NTPase} \quad (3)$$

where K_{path} is the molar absorption coefficient for NADH for a given optical path length, which was calculated to be 3,965.75 OD units mol^{-1} for the assay volume (75 μl) in 384-well clear-bottom assay plates (Corning) used in the assay. dA_{350}/dt was corrected for background NADH hydrolysis and NTP hydrolysis by subtracting a no-protein control from all experimental data points.

Final NTPase assay conditions (75 μl reaction volume) were as follows: 100 nM pCU1 TraI, 1.25 mM NTP, 100 nM single-stranded DNA (ssDNA), 0.7 mM phosphoenolpyruvate (PEP), 0.3 mM NADH, 50 mM PK, and 50 mM LDH. TraI, ssDNA, and NTPs were diluted into ATPase buffer (buffer P) consisting of 25 mM NaCl, 50 mM Tris acetate (pH 7.5), 10 mM magnesium acetate, 25 mM K_2PO_4, and 0.1 mg/ml of bovine serum albumin (BSA) prior to use in the assay. pCU1 TraI was allowed to bind to the ssDNA for 10 min at 37°C prior to the addition of NTP. Upon addition of NTP, dA_{350} was monitored for 2.5 h at 37°C. All reagents, including enzymes and NTPs, were acquired from Sigma-Aldrich. ssDNA substrates used in the assays were obtained commercially from IDT and initially resuspended in buffer R (50 mM NaCl, 10 mM Tris-HCl [pH 7.5], 0.05 mM EDTA, 0.01% azide). The DNA nucleotide sequences used are listed in Table 1.

EMSAs. Electrophoretic mobility shift assays (EMSAs) were used to visualize the helicase activity of TraI by detecting the ability of TraI to displace a labeled DNA fragment from a partial duplex DNA molecule. TraI constructs were incubated in the presence of ATP with a double-stranded DNA substrate (17-mer–80-mer), consisting of one unlabeled strand (80-mer) and one fluorescein-labeled strand (17-mer). After the reactions were quenched, a gel was used to visualize substrates and products. TraI unwinding activity was assessed by the presence of a smaller product band on the gel, corresponding to the unwound 17-mer.

Helicase reaction mixtures contained 3.5 to 8 μM TraI, 0.5 μM DNA substrate (17-mer–80-mer), 5 μM trap DNA, 2.5 mM ATP, 33 mM Tris acetate (pH 7.5), 1% dimethyl sulfoxide, and 10 mM β-mercaptoethanol. DNA substrates were commercially synthesized by IDT and resuspended in buffer R (50 mM NaCl, 10 mM Tris-HCl [pH 7.5], 0.05 mM EDTA, 0.01% azide). The DNA nucleotide sequences used are listed in Table 1. To anneal the 17-mer–80-mer DNA substrate, ssDNA strands were mixed in an equimolar ratio, heated to 95°C for 10 min, and then allowed to slowly cool to room temperature. TraI was diluted into buffer Q (15 mM HEPES [pH 7.5], 20 mM NaCl, 0.1 mg/ml of BSA, 0.3 mM $MgCl_2$) prior to use in the assay.

Time course helicase assay mixtures were incubated at 37°C and quenched at the desired time with the addition of 5 μl of 10% SDS and 4 μl of loading dye. The reaction volume was 300 μl, with a starting TraI concentration of 3.5 μM. Aliquots (20 μl) were removed and quenched at 1, 5, 15, 30, 45, 60, and 120 min. At 60 min, a parallel reaction was initiated by removing 130 μl of the initial reaction product and doubling the TraI concentration to 7 μM. Aliquots (20 μl) were removed from the second reaction mixture and quenched at the time points indicated above. Helicase assay mixtures of TraI constructs (8 μM) with or without the extreme C terminus (20-μl reaction volume) were incubated at 37°C and quenched at 30 min.

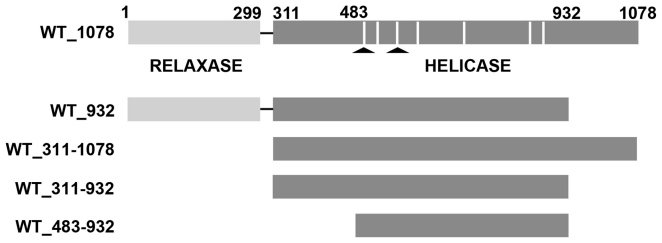

FIG 2 pCU1 TraI domain organization and protein constructs used in this study. Wild-type TraI has 1,078 amino acids (WT_1078). The N-terminal region contains the relaxase domain between residues 1 and 299, while the C-terminal region harbors a predicted helicase domain. Canonical helicase motifs (white boxes) span a region between residues 498 and 894. Residue ranges for each TraI deletion construct used are indicated. Filled triangles represent the location of point mutations in conserved helicase motifs investigated in full-length TraI.

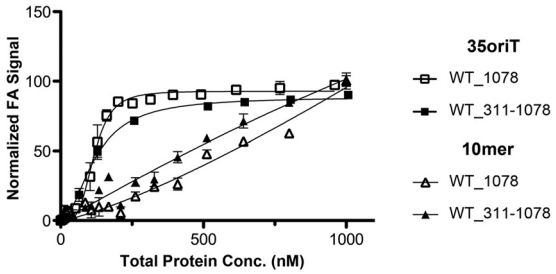

FIG 3 pCU1 TraI DNA binding activity. Representative fluorescence anisotropy curves with standard error bars for wild-type pCU1 TraI (WT_1078) and TraI helicase (WT_311-1078) constructs binding to 35oriT and 10-mer DNA substrates. The DNA binding curves generated by WT_1078 and WT_311-1078 were best fit by sigmoidal and hyperbolic fits, respectively.

Samples (20 μl) of each quenched helicase reaction were run through a 17% polyacrylamide gel (17 ml of 40% polyacrylamide-bisacrylamide [37:1], 2 ml of 10× Tris-borate-EDTA [TBE], 400 μl of 10% SDS, 300 μl of 10% ammonium persulfate [APS], 30 μl of tetramethylethylenediamine [TEMED]) in TBE running buffer (0.5× TBE, 0.1% SDS) to separate the substrate and products. The gel was run for 160 min at 20 mA, with an attached ice pack to avoid overheating effects. The fluorescent oligonucleotides were visualized using Quantity One software and a VersaDoc imaging system (Bio-Rad). Band intensities were quantified using ImageJ v1.42 (W. S. Rasband, NIH, 2008). Unwinding activity was reported as the percentage of substrate unwound (fragment displacement): the product band intensity was divided by the sum of the product band plus substrate band intensities and then multiplied by 100%.

RESULTS

TraI contains conserved SF1 helicase motifs. Initiation of conjugative plasmid transfer (CPT) requires the binding and nicking of the conjugative DNA plasmid's origin of transfer (*oriT*) by the relaxase enzyme (3, 56, 57). For DNA strand transfer to occur after the *oriT* is nicked, helicase activity is essential (19–21, 24, 56). Helicase activity involves DNA binding, NTP hydrolysis, and the coupling of this hydrolysis to the unwinding of dsDNA substrates (1, 2, 22). The conjugative proteins TraI and TrwC, from MOB_F conjugative plasmids F and R388, respectively, have N-terminal relaxases and C-terminal helicases (23, 38, 39, 41, 44) and are functionally homologous to pCU1 TraI (24, 50, 56). Sequence alignment of the predicted pCU1 TraI helicase region with the helicase regions of F TraI and R388 TrwC provisionally identified seven conserved superfamily 1 (SF1) helicase motifs within the pCU1 sequence (I to VI) (Fig. 1) (1, 2, 25–27). Further inspection of the pCU1 sequence identified specific residues within these motifs associated with helicase activity, including an invariant lysine (Lys-507) in motif I/Walker A, the DExx box in motif II/Walker B (Asp-568 and Glu-569), and a conserved arginine (Arg-696) in motif IV, further suggesting that TraI was indeed an active helicase (1, 2, 24, 28–30).

TraI helicase binds with high affinity to *oriT* DNA. We first examined the ability of pCU1 TraI helicase constructs to bind several DNA substrates (Table 1) using fluorescence anisotropy-based DNA binding assays. DNA substrates were fluorescently labeled, and the change in the substrate's fluorescence anisotropy was monitored as a function of increasing protein concentration. Only pCU1 TraI constructs containing the predicted helicase motifs were examined (Fig. 2): full-length TraI (WT_1078), TraI with a C-terminal truncation after the conserved helicase motif (WT_932; for clarity, residues 933 to 1078 are henceforth referred to as the extreme C terminus), the entire C-terminal domain (WT_311-1078), a C-terminal domain lacking the extreme C terminus (WT_311-932), and a "minimal helicase domain" containing only the predicted helicase motifs (WT_483-932). The panel of DNA substrates included three of the same length (35 nucleotides) to examine the role of structure and sequence DNA binding by the TraI C terminus: (i) 35oriT, which consisted of the hairpin-forming origin of transfer sequence from plasmid pCU1; (ii) 35-mer-hairpin, a substrate with structural, but no sequence, similarity to 35oriT; and (iii) a 35-mer substrate with no sequence or structural similarity to 35oriT (Table 1). All TraI constructs bound these DNA substrates with similar affinities ranging from 58 to 180 nM (Table 2; Fig. 3, squares). The largest increase in affinity occurred when the relaxase region was absent (WT_311-1078, WT_311-932, and WT_483-932) (Table 2), although this was maximally a 3-fold difference that was not consistent across all

TABLE 2 Summary of pCU1 TraI DNA binding activities

TraI construct	K_D (nM) for DNA substrate[a]				
	35oriT-hairpin	35-mer-hairpin	35-mer	19-mer	10-mer
WT_1078[b]	117 ± 3	59 ± 2	79 ± 2	106 ± 4	ND
WT_932[b]	58 ± 1	80 ± 2	97 ± 2	—	—
WT_311-1078	102 ± 9	194 ± 8	107 ± 7	408 ± 22	ND
WT_311-932[b]	137 ± 3	180 ± 3	176 ± 2	—	—
WT_483-932	138 ± 18	138 ± 18	145 ± 19	—	—

[a] Average values of three independent experiments. Standard errors are indicated. ND, binding experiment was performed but no binding was observed. —, this binding experiment was not performed.
[b] Data fit with equation 2 to yield an apparent K_D.

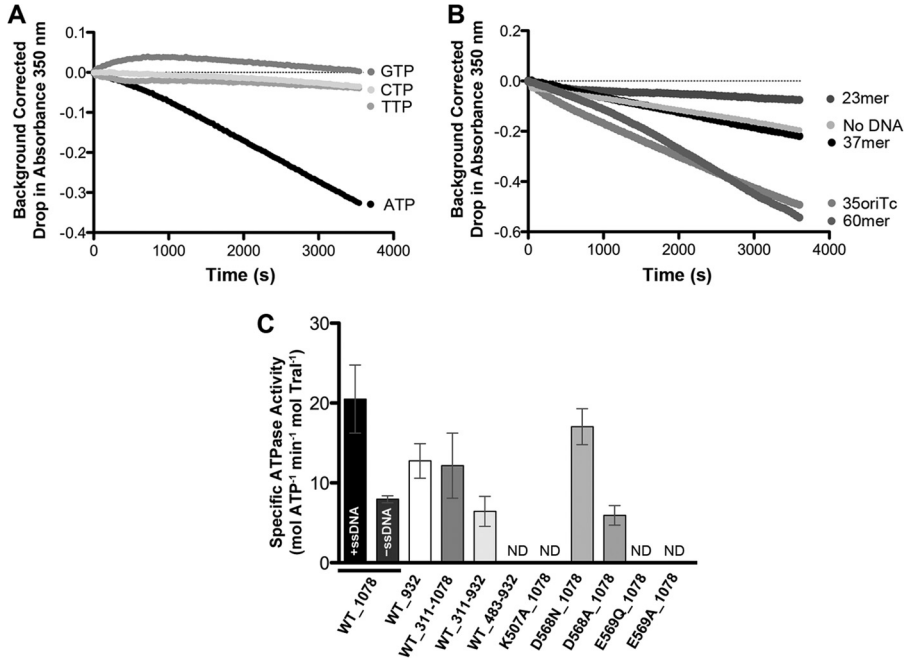

FIG 4 pCU1 TraI NTPase activity. (A) NTP hydrolysis by TraI. Hydrolysis is indicated by a reduction in absorbance at 350 nm and was observed only in the presence of ATP. Little or no activity was observed in the presence of TTP, GTP, and CTP. All reaction mixtures contained 100 nM 60-mer ssDNA. (B) Influence of ssDNA length on the ATPase activity of TraI. TraI exhibits low background ATPase activity in the absence of DNA. An increase in activity was seen as the ssDNA length increased from 37 to 60 nucleotides, whereas a shorter substrate reduced activity. Similar activity was seen for the 60-nucleotide substrate and the shorter 35oriTc (Table 1), indicating some sequence specificity. All DNA substrate concentrations were 500 nM. (For clarity, averages of three experiments each are shown and error bars are omitted from panels A and B.) (C) ATPase activity of full-length TraI, deletion mutants, and ATPase motif mutants. Deletion mutant constructs containing at least residues 311 to 932 retained ATPase activity. Point mutations in the conserved helicase motif residues K507 and E569 eliminated ATPase activity, while constructs with substitutions at residue D568 retained all or some ATPase activity. Error bars represent standard errors between at least two independent experiments. ND, not detected.

three DNA substrates. When removed from the context of the full-length protein, the TraI relaxase is also able to bind these DNA substrates, though at a much lower affinity (~1 μM [31–35, 53]). The presence of the relaxase domain does not appear to impact significantly the overall DNA binding activity of pCU1 TraI. Removal of the extreme C terminus also did not significantly impact DNA binding ability, as WT_932 and WT_311-932 bound to DNA substrates with affinities similar to that of full-length TraI (Table 2).

To investigate the effect of substrate length on DNA binding affinity by TraI, two shorter DNA substrates (19-mer and 10-mer) were evaluated. WT_1078 bound with high affinity to the 19-mer substrate (106 nM) (Table 2), while the C-terminal construct (WT_311-1078) bound with slightly weaker affinity (408 nM) (Table 2). We were unable to determine affinities for the 10-mer DNA substrate with either WT_1078 or WT_311-1078 due to poor binding (Fig. 3, triangles).

The DNA binding curves generated by the various full-length and C-terminal TraI constructs were either sigmoidal or hyperbolic in appearance (Fig. 3, open squares and closed squares, respectively). Equation 1 was used to fit the sigmoidal curves (WT_1078, WT_932, and WT_932) generating an apparent K_D, whereas hyperbolic curves (WT_311-1078 and WT_483-1078) were fit with equation 2. As the apparent K_D is an approximate measure, the actual binding affinity of TraI helicase constructs for the DNA substrates may be underestimated. The sigmoidal curve shape is likely a result of independent binding of the relaxase and helicase domains or a result of multiple TraI molecules binding to the DNA substrate. However, analysis by size exclusion chromatography and static light scattering (SEC-SLS) indicated that a 1:1 ratio of DNA to TraI is favored for the 35oriT DNA and wild-type TraI (data not shown). While shorter constructs, such as WT_311-932, may bind in a different ratio to the DNA substrates, giving rise to the seemingly cooperative binding, it is most likely that TraI binds DNA as a monomer and cooperativity is due to the presence of two DNA binding domains, the relaxase and helicase.

TraI NTPase activity. Wild-type TraI was assessed for nucleotide triphosphate (NTP) hydrolysis activity using an NADH-linked enzyme assay) (see Materials and Methods and reference 55). In the presence of ssDNA (60-mer; 100 nM), we investigated the ability of TraI to hydrolyze the four standard NTP substrates: ATP, GTP, CTP, and TTP. NTP hydrolysis was observed only with ATP (Fig. 4A). However, since the enzymatic activity of pyruvate kinase is known to be more stimulated in the presence of ATP than with other NTPs (29, 36, 58), pCU1 TraI may have some limited activity in the presence of other NTPs. Since the ATPase activity of many SF1B helicases is stimulated by ssDNA, we assessed the influence of ssDNA length on the ATPase activity of TraI. Three ssDNA substrates (500 nM) of increasing lengths (23, 37, and 60 nucleotides) (Table 1) were tested. As the length of DNA increased from 37 to 60 nucleotides, the rate of ATPase activity also increased (Fig. 4B); however, the substrate shorter than 37 nucleotides seemed to inhibit ATPase activity. Additionally, we tested the single-stranded complement of the 35oriT (35oriTc) and found

that it stimulated TraI ATPase activity similarly to the 60-nucleotide ssDNA substrate, indicating some sequence specificity (Fig. 4B). We found that in the absence of ssDNA, TraI has some low ATPase activity (Fig. 4B and C).

We examined the ATPase activity in the presence of ssDNA of the TraI full-length wild type (WT_1078), as well as constructs containing only the predicted helicase domains (WT_483-932), lacking the extreme C terminus (WT_932) or lacking the relaxase domain (WT_311-1078), or both (WT_311-932) (Fig. 4C). The shortest construct, WT_483-932, possessed no observable ATPase activity. Since WT_483-932 still retains DNA binding activity (Table 2), residues 311 to 482 are thus essential for ATPase activity. Compared to the specific ATPase activity of WT_1078 (21 ± 4 mol of ATP min^{-1} mol of $TraI^{-1}$), the activities for WT_932 and WT_311-1078 were not significantly affected (13 ± 2 and 12 ± 4 mol of ATP min^{-1} mol of $TraI^{-1}$, respectively). WT_932 demonstrated a specific ATPase activity that was less than 2-fold lower than wild-type TraI activity, indicating that the loss of the C terminus does not significantly affect the ATPase activity (Fig. 4C). The specific ATPase activity of WT_311-1078 was indistinguishable from that of WT_932, suggesting that in the context of the full-length protein, the relaxase domain may only slightly enhance the overall ATPase activity of TraI (Fig. 4C). Though retaining ATPase activity, WT_311-932, which lacks both the relaxase domain and the extreme C terminus, hydrolyzed ATP at the level observed for full-length TraI in the absence of ssDNA (7 ± 2 mol of ATP min^{-1} mol of $TraI^{-1}$) (Fig. 4C), indicating an apparent loss of the ssDNA-stimulated ATPase activity.

Motifs I and II (Walker A and Walker B) are highly conserved across SF1 and SF2 helicases (1, 37). Point mutations were made to key residues within these motifs in pCU1 TraI, and their impact on ATPase activity was measured (Fig. 4C). Mutation of the conserved lysine in the Walker A motif, which coordinates phosphates of the bound ATP substrate (1, 29, 35, 37), to alanine (K507A) eliminated ATPase activity (Fig. 4C). Mutations similar to the conserved DExx box residues within the Walker B motif eliminated or significantly reduced pCU1 TraI activity. For example, mutation of conserved aspartic acid and glutamic acid residues that are expected to coordinate the Mg^{2+} ion and serve as a catalytic base, respectively, reduced (D568A; 6 ± 1 mol of ATP min^{-1} mol of $TraI^{-1}$) or eliminated (E569A) ATPase activity. However, an aspartic acid-to-asparagine mutation (D568N) had no effect on the ATPase activity (17 ± 2 mol of ATP min^{-1} mol of $TraI^{-1}$).

The TraI C terminus is required for efficient unwinding *in vitro*. Wild-type TraI (WT_1078) was assayed for DNA strand separation, or unwinding, activity using electrophoretic mobility shift assays (Fig. 5). In the presence of ATP, WT_1078 unwound a portion of the dsDNA substrate; however, fragment displacement began to plateau around 30 min and maintained ~30% of substrate unwound (Fig. 5A, closed circles). Increasing the TraI concentration after initial unwinding had leveled off (Fig. 5A, open circles) led to continued fragment displacement, from ~30% to ~60% of substrate unwound (Fig. 5A).

The shorter TraI constructs that were found to retain ATPase activity (WT_932, WT_311-1078, and WT_311-932) were also assayed for unwinding activity using a 30-min incubation period (Fig. 5B and C). Surprisingly, WT_932 showed a significant reduction in unwinding activity, with less than one-fifth the level of unwound substrate observed with the full-length enzyme (4% versus 37% unwound) (Fig. 5C). WT_311-1078 unwound dsDNA

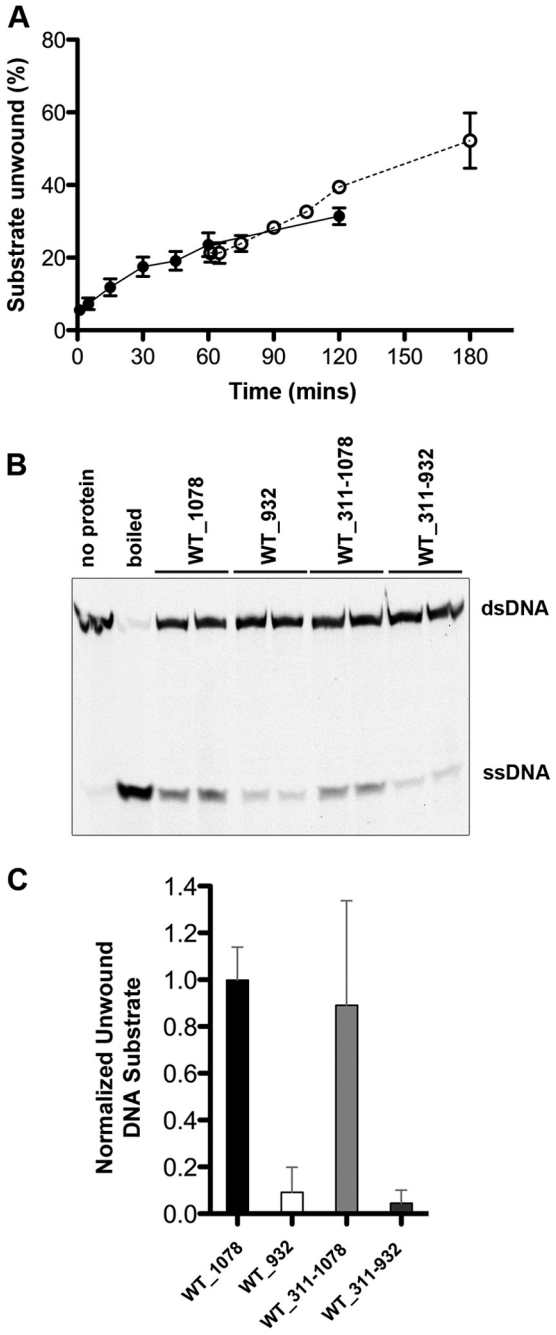

FIG 5 pCU1 TraI dsDNA separation activity. (A) Kinetics of the unwinding reaction at different TraI concentrations. The time course of the pCU1 TraI unwinding reaction using the partial duplex 17-mer–80-mer dsDNA substrate is shown. Helicase assays were performed at 37°C as described in Materials and Methods with a starting TraI concentration of 3.5 μM (●), which was then increased to 7 μM (○). Standard error between multiple experiments is shown. (B) Representative electrophoretic mobility shift assay. dsDNA strand separation by TraI constructs with or without the extreme C terminus (residues 933 to 1078) was measured with EMSA. The TraI construct used is indicated, and each reaction was run in duplicate. Helicase assays were performed at 37°C for 30 min with 8 μM TraI and 0.5 μM dsDNA substrate as described in Materials and Methods. (C) Bar graph of normalized unwinding activity for each TraI construct tested, with standard error shown. Percent dsDNA fragment unwound was normalized to wild-type levels. TraI constructs lacking the extreme C terminus have significantly reduced ability to unwind the 17-mer–80-mer dsDNA substrate (see Table 1 for sequence information).

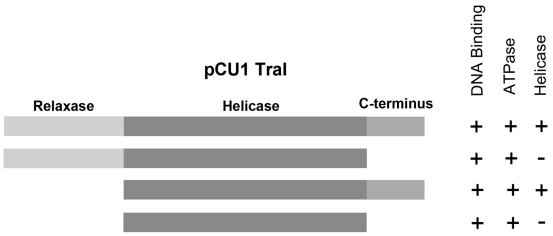

FIG 6 Dissection of functional domains of pCU1 TraI. All pCU1 constructs have DNA binding ability. Those lacking the N-terminal relaxase retain both ATPase and DNA unwinding activities (+). However, constructs lacking the extreme C terminus (residues 933 to 1078) are unable to unwind dsDNA substrates efficiently (−).

substrate at a rate comparable to that of the full-length enzyme (33% unwound), while WT_311-932 performed similarly to WT_932, with almost all of the substrate left (2% unwound) (Fig. 5C). In the absence of ATP, WT_1078 had no observable unwinding activity (data not shown), demonstrating that ATP hydrolysis is necessary for unwinding. Reduced unwinding activity was observed for constructs lacking the extreme C terminus, WT_932 and WT_311-932, compared to that of the wild type (WT_1078). The presence or absence of the relaxase domain (WT_932 or WT_311-1078, respectively) did not seem to influence the unwinding activity, as WT_311-1078 unwound substrate at wild-type levels. These data support the conclusion that the extreme C terminus of pCU1 TraI provides an essential dsDNA unwinding function required for the conjugative transfer of the pCU1 plasmid.

DISCUSSION

The TraI protein is essential for conjugative transfer of plasmid pCU1, a member of the MOB_F family of conjugative plasmids (38, 39, 50). The N-terminal region encodes a relaxase enzyme with transesterase activity (40, 41, 53), while the C-terminal region contains a predicted helicase domain (Fig. 1 and 2). Homologous bifunctional conjugative proteins F TraI and TrwC, from MOB_F conjugative plasmids F and R388, respectively, also each have an N-terminal relaxase and C-terminal helicase (38, 39, 41–46, 59). Though the transesterase activity of the pCU1 TraI N-terminal relaxase has been extensively studied (53, 54), in this study we identified key residues and motifs utilized by the pCU1 TraI helicase, determined the extent of the helicase domain, and elucidated the nature of its DNA binding, ATPase, and DNA strand separation activities (Fig. 6).

pCU1 TraI C-terminal helicase constructs bound DNA substrates with nanomolar binding affinity (Table 2), comparable to that of full-length TraI (WT_1078) (Table 2; Fig. 6), illustrating that the pCU1 TraI relaxase does not enhance the affinity of pCU1 TraI for DNA substrates. In contrast, R1 TraI, which is closely related to F plasmid TraI (24, 38, 44, 48), exhibits a 10-fold reduction in DNA binding affinity in the absence of its N-terminal relaxase relative to full-length R1 TraI levels (48, 49). Additionally, unlike analogous pCU1 construct WT_483-932, an F TraI helicase construct containing all the functional helicase motifs lacked detectable DNA binding affinity; the high-affinity DNA binding site is instead located in a separate specialized RecD-like domain (48, 50–52). Furthermore, the binding affinities of these pCU1 C-terminal constructs showed no dependence on DNA sequence, DNA secondary structure, or similarity of the DNA substrate to the pCU1 *oriT* DNA (Table 2; Fig. 6). In contrast, DNA binding by both the relaxase and helicase domains of F TraI shows some degree of sequence specificity (48, 53, 54). These findings for the pCU1 TraI helicase domain mirror those reported by Nash et al. (53) for the pCU1 TraI relaxase domain, which also did not demonstrate significant DNA sequence or structure specificity for binding. pCU1 TraI likely functions in coordination with an additional plasmid-encoded factor, such as pCU1 TraK, to ensure plasmid specificity during conjugative plasmid transfer, as previously suggested (53). The minimum TraI DNA binding site is greater than 10 nucleotides in length, as no significant DNA binding to the 10-mer DNA substrate was observed (Fig. 3; Table 2). Many SF1 and SF2 helicase structures contain a DNA binding site of 8 to 10 nucleotides (1).

ATPase activity and strand separation activity were observed in full-length pCU1 TraI and several C-terminal helicase constructs. pCU1 TraI exhibited basal ATPase activity that was stimulated by ssDNA, with length dependence and some sequence specificity for stimulation. The rates of ATP hydrolysis by pCU1 TraI were 150- and 350-fold, respectively, lower than those by TrwC and F TraI (28, 60). Strand separation assays show that the pCU1 TraI rate of unwinding levels off over time (Fig. 5A), as similarly observed with TrwC, and suggest a slow turnover rate (28). The minimal functional pCU1 TraI helicase extends from residues 311 to 1078 and can accomplish DNA binding, ATP hydrolysis, and DNA unwinding. Smaller constructs lack ATPase or DNA unwinding activity, but all constructs retain DNA binding activity. For example, WT_483-932 contains all the conserved helicase motifs, but this construct was unable to hydrolyze ATP in spite of the fact that its DNA binding ability remained intact (Table 2). Available structural data suggest that residues 311 to 482 will form part of the core RecA-like domain in the pCU1 TraI helicase structure (19, 21, 61), so deletion of these residues is likely to be detrimental to function, as we have demonstrated. A slightly larger construct, WT_311-932, demonstrated some ATPase activity (Fig. 4C) and DNA binding activity (Table 2) but, surprisingly, was unable to unwind DNA (Fig. 5B and C). Interestingly, WT_932, which lacks only the extreme C terminus (residues 933 to 1078), also suffered a loss in unwinding activity similar to that suffered by WT_311-932 but maintained wild-type levels of ATPase activity (Fig. 4C and 5C). With WT_311-932, the ATPase activity observed was at the basal ATPase activity observed for TraI in the absence of DNA, indicating that ssDNA-stimulated ATPase activity is lost when both the relaxase and extreme C terminus are absent. Of note, the isolated extreme C terminus (residues 933 to 1078) has no observable ability to bind DNA, single or double stranded (data not shown), suggesting that this loss in ssDNA-stimulated activity is not due to loss of any DNA binding. Lacking only the relaxase domain, WT_311-1078 both hydrolyzed ATP and unwound dsDNA substrates at wild-type levels, pointing to a crucial role for these extreme C-terminal residues in pCU1 TraI helicase function.

Previous studies have shown that deletion of the F TraI extreme C-terminal domain leads to loss of conjugative plasmid transfer. Of note, however, unlike pCU1 TraI, this deletion does not significantly affect the ability of the helicase to hydrolyze ATP or unwind substrates (39, 62). Thus, we suggest that this pCU1 TraI C terminus be considered a distinct functional domain in this enzyme (Fig. 6) and, relative to other relaxase-helicase proteins examined to date, one that is essential for linking ATP hydrolysis

to strand separation, ensuring helicase function during conjugation.

ACKNOWLEDGMENTS

This work was supported by National Institutes of Health grant AI078924 to M.R.R.; in addition, K.J.M. was supported by a grant from the National Institute of General Medical Sciences, division of Training, Workforce Development, and Diversity under the Institutional Research and Academic Career Development Award, grant K12-GM000678.

REFERENCES

1. **Caruthers JM, McKay DB.** 2002. Helicase structure and mechanism. Curr. Opin. Struct. Biol. **12:**123–133. http://dx.doi.org/10.1016/S0959-440X(02)00298-1.
2. **Hall MC, Matson SW.** 1999. Helicase motifs: the engine that powers DNA unwinding. Mol. Microbiol. **34:**867–877. http://dx.doi.org/10.1046/j.1365-2958.1999.01659.x.
3. **Singleton MR, Dillingham MS, Wigley DB.** 2007. Structure and mechanism of helicases and nucleic acid translocases. Annu. Rev. Biochemistry **76:**23–50. http://dx.doi.org/10.1146/annurev.biochem.76.052305.115300.
4. **Delagoutte E, von Hippel PH.** 2003. Helicase mechanisms and the coupling of helicases within macromolecular machines. Part II: integration of helicases into cellular processes. Q. Rev. Biophys. **36:**1–69. http://dx.doi.org/10.1017/S0033583502003864.
5. **Lohman TM, Tomko EJ, Wu CG.** 2008. Non-hexameric DNA helicases and translocases: mechanisms and regulation. Nat. Rev. Mol. Cell Biol. **9:**391–401. http://dx.doi.org/10.1038/nrm2394.
6. **Patel SS, Donmez I.** 2006. Mechanisms of helicases. J. Biol. Chem. **281:**18265–18268. http://dx.doi.org/10.1074/jbc.R600008200.
7. **Chen C-S, Chiou C-T, Chen GS, Chen S-C, Hu C-Y, Chi W-K, Chu Y-D, Hwang L-H, Chen P-J, Chen D-S, Liaw S-H, Chern J-W.** 2009. Structure-based discovery of triphenylmethane derivatives as inhibitors of hepatitis C virus helicase. J. Med. Chem. **52:**2716–2723. http://dx.doi.org/10.1021/jm8011905.
8. **Kandil S, Biondaro S, Vlachakis D, Cummins A-C, Coluccia A, Berry C, Leyssen P, Neyts J, Brancale A.** 2009. Discovery of a novel HCV helicase inhibitor by a de novo drug design approach. Bioorg. Med. Chem. Lett. **19:**2935–2937. http://dx.doi.org/10.1016/j.bmcl.2009.04.074.
9. **Phoon CW, Ng PY, Ting AE, Yeo SL, Sim MM.** 2001. Biological evaluation of hepatitis C virus helicase inhibitors. Bioorg. Med. Chem. Lett. **11:**1647–1650. http://dx.doi.org/10.1016/S0960-894X(01)00263-3.
10. **Crute JJ, Grygon CA, Hargrave KD, Simoneau B, Faucher A-M, Bolger G, Kibler P, Liuzzi M, Cordingley MG.** 2002. Herpes simplex virus helicase-primase inhibitors are active in animal models of human disease. Nat. Med. **8:**386–391. http://dx.doi.org/10.1038/nm0402-386.
11. **Kleymann G, Fischer R, Betz UAK, Hendrix M, Bender W, Schneider U, Handke G, Eckenberg P, Hewlett G, Pevzner V, Baumeister J, Weber O, Henninger K, Keldenich J, Jensen A, Kolb J, Bach U, Popp A, Maben J, Frappa I, Haebich D, Lockhoff O, Rubsamen-Waigmann H.** 2002. New helicase-primase inhibitors as drug candidates for the treatment of herpes simplex disease. Nat. Med. **8:**392–398. http://dx.doi.org/10.1038/nm0402-392.
12. **Aiello D, Barnes MH, Biswas EE, Biswas SB, Gu S, Williams JD, Bowlin TL, Moir DT.** 2009. Discovery, characterization and comparison of inhibitors of Bacillus anthracis and Staphylococcus aureus replicative DNA helicases. Bioorg. Med. Chem. **17:**4466–4476. http://dx.doi.org/10.1016/j.bmc.2009.05.014.
13. **Aggarwal M, Sommers JA, Shoemaker RH, Brosh RM.** 2011. Inhibition of helicase activity by a small molecule impairs Werner syndrome helicase (WRN) function in the cellular response to DNA damage or replication stress. Proc. Natl. Acad. Sci. U. S. A. **108:**1525–1530. http://dx.doi.org/10.1073/pnas.1006423108.
14. **Griep MA, Blood S, Larson MA, Koepsell SA, Hinrichs SH.** 2007. Myricetin inhibits Escherichia coli DnaB helicase but not primase. Bioorg. Med. Chem. **15:**7203–7208. http://dx.doi.org/10.1016/j.bmc.2007.07.057.
15. **McKay GA, Reddy R, Arhin F, Belley A, Lehoux D, Moeck G, Sarmiento I, Parr TR, Gros P, Pelletier J, Far AR.** 2006. Triaminotriazine DNA helicase inhibitors with antibacterial activity. Bioorg. Med. Chem. Lett. **16:**1286–1290. http://dx.doi.org/10.1016/j.bmcl.2005.11.076.
16. **Zhang B, Zhang A-H, Chen L, Xi XG.** 2008. Inhibition of DNA helicase, ATPase and DNA-binding activities of E. coli RecQ helicase by chemotherapeutic agents. J. Biochem. **143:**773–779.
17. **Chono K, Katsumata K, Kontani T, Kobayashi M, Suo K, Yokota T, Konno K, Shimizu Y, Suzuki H.** 2010. ASP2151, a novel helicase-primase inhibitor, possesses antiviral activity against varicella-zoster virus and herpes simplex virus types 1 and 2. J. Antimicrob. Chemother. **65:**1733–1741. http://dx.doi.org/10.1093/jac/dkq198.
18. **Aggarwal M, Brosh RM.** 2009. Hitting the bull's eye: novel directed cancer therapy through helicase-targeted synthetic lethality. J. Cell. Biochem. **106:**758–763. http://dx.doi.org/10.1002/jcb.22048.
19. **Saikrishnan K, Powell B, Cook NJ, Webb MR, Wigley DB.** 2009. Mechanistic basis of 5′-3′ translocation in SF1B helicases. Cell **137:**849–859. http://dx.doi.org/10.1016/j.cell.2009.03.036.
20. **He X, Byrd AK, Yun M-K, Pemble CW, Harrison D, Yeruva L, Dahl C, Kreuzer KN, Raney KD, White SW.** 2012. The T4 phage SF1B helicase Dda is structurally optimized to perform DNA strand separation. Structure **20:**1189–1200. http://dx.doi.org/10.1016/j.str.2012.04.013.
21. **Saikrishnan K, Griffiths SP, Cook N, Court R, Wigley DB.** 2008. DNA binding to RecD: role of the 1B domain in SF1B helicase activity. EMBO J. **27:**2222–2229. http://dx.doi.org/10.1038/emboj.2008.144.
22. **Gu J, Xia X, Yan P, Liu H, Podust VN, Reynolds AB, Fanning E.** 2004. Cell cycle-dependent regulation of a human DNA helicase that localizes in DNA damage foci. Mol. Biol. Cell **15:**3320–3332. http://dx.doi.org/10.1091/mbc.E04-03-0227.
23. **Boulé J-B, Vega LR, Zakian VA.** 2005. The yeast Pif1p helicase removes telomerase from telomeric DNA. Nature **438:**57–61. http://dx.doi.org/10.1038/nature04091.
24. **Matson SW, Sampson JK, Byrd DR.** 2001. F plasmid conjugative DNA transfer: the TraI helicase activity is essential for DNA strand transfer. J. Biol. Chem. **276:**2372–2379. http://dx.doi.org/10.1074/jbc.M008728200.
25. **Mazel D, Davies J.** 1999. Antibiotic resistance in microbes. Cell. Mol. Life Sci. **56:**742–754. http://dx.doi.org/10.1007/s000180050021.
26. **Waters VL.** 1999. Conjugative transfer in the dissemination of beta-lactam and aminoglycoside resistance. Front. Biosci. **4:**D433–D456. http://dx.doi.org/10.2741/Waters.
27. **Alekshun MLS.** 2007. Molecular mechanisms of antibacterial multidrug resistance. Cell **128:**1037–1050. http://dx.doi.org/10.1016/j.cell.2007.03.004.
28. **Grandoso G, Llosa M, Zabala JC, de la Cruz F.** 1994. Purification and biochemical characterization of TrwC, the helicase involved in plasmid R388 conjugal DNA transfer. FEBS J. **226:**403–412.
29. **de la Cruz F, Frost LS, Meyer RJ, Zechner EL.** 2010. Conjugative DNA metabolism in Gram-negative bacteria. FEMS Microbiol. Rev. **34:**18–40. http://dx.doi.org/10.1111/j.1574-6976.2009.00195.x.
30. **Cheng Y, McNamara DE, Miley MJ, Nash RP, Redinbo MR.** 2011. Functional characterization of the multidomain F plasmid TraI relaxase-helicase. J. Biol. Chem. **286:**12670–12682. http://dx.doi.org/10.1074/jbc.M110.207563.
31. **Willetts N, Skurray R.** 1980. The conjugation system of F-like plasmids. Annu. Rev. Genet. **14:**41–76. http://dx.doi.org/10.1146/annurev.ge.14.120180.000353.
32. **Ippen-Ihler KA, Minkley EG.** 1986. The conjugation system of F, the fertility factor of Escherichia coli. Annu. Rev. Genet. **20:**593–624. http://dx.doi.org/10.1146/annurev.ge.20.120186.003113.
33. **Arutyunov D, Frost LS.** 2013. F conjugation: back to the beginning. Plasmid **70:**18–32. http://dx.doi.org/10.1016/j.plasmid.2013.03.010.
34. **Francia MV, Varsaki A, Garcillan-Barcia MP, Latorre A, Drainas C, de la Cruz F.** 2004. A classification scheme for mobilization regions of bacterial plasmids. FEMS Microbiol. Rev. **28:**79–100. http://dx.doi.org/10.1016/j.femsre.2003.09.001.
35. **Garcillán-Barcia MP, Francia MV, de la Cruz F.** 2009. The diversity of conjugative relaxases and its application in plasmid classification. FEMS Microbiol. Rev. **33:**657–687. http://dx.doi.org/10.1111/j.1574-6976.2009.00168.x.
36. **Willetts N, Wilkins B.** 1984. Processing of plasmid DNA during bacterial conjugation. Microbiol. Rev. **48:**24–41.
37. **Smillie C, Garcillan-Barcia MP, Francia MV, Eduardo Rocha PC, de la Cruz F.** 2010. Mobility of plasmids. Microbiol. Mol. Biol. Rev. **74:**434–452. http://dx.doi.org/10.1128/MMBR.00020-10.
38. **Llosa M, Grandoso G, Hernando MA, de la Cruz F.** 1996. Functional domains in protein TrwC of plasmid R388: dissected DNA strand transferase and DNA helicase activities reconstitute protein function. J. Mol. Biol. **264:**56–67. http://dx.doi.org/10.1006/jmbi.1996.0623.
39. **Matson SW, Ragonese H.** 2005. The F-plasmid TraI protein contains three functional domains required for conjugative DNA strand trans-

fer. J. Bacteriol. **187:**697–706. http://dx.doi.org/10.1128/JB.187.2.697-706.2005.
40. **Datta S, Larkin C, Schildbach JF.** 2003. Structural insights into single-stranded DNA binding and cleavage by F factor TraI. Structure **11:**1369–1379. http://dx.doi.org/10.1016/j.str.2003.10.001.
41. **Guasch A, Lucas M, Moncalian G, Cabezas M, Perez-Luque R, Gomis-Ruth FX, de la Cruz F, Coll M.** 2003. Recognition and processing of the origin of transfer DNA by conjugative relaxase TrwC. Nat. Struct. Biol. **10:**1002–1010. http://dx.doi.org/10.1038/nsb1017.
42. **Boer R, Russi S, Guasch A, Lucas M, Blanco AG, Perez-Luque R, Coll M, de la Cruz F.** 2006. Unveiling the molecular mechanism of a conjugative relaxase: the structure of TrwC complexed with a 27-mer DNA comprising the recognition hairpin and the cleavage site. J. Mol. Biol. **358:**857–869. http://dx.doi.org/10.1016/j.jmb.2006.02.018.
43. **Gonzalez-Perez B, Lucas M, Cooke LA, Vyle JS, de la Cruz F, Moncalian G.** 2007. Analysis of DNA processing reactions in bacterial conjugation by using suicide oligonucleotides. EMBO J. **26:**3847–3857. http://dx.doi.org/10.1038/sj.emboj.7601806.
44. **Byrd DR, Matson SW.** 1997. Nicking by transesterification: the reaction catalysed by a relaxase. Mol. Microbiol. **25:**1011–1022. http://dx.doi.org/10.1046/j.1365-2958.1997.5241885.x.
45. **Larkin C, Haft RJ, Harley MJ, Traxler B, Schildbach JF.** 2007. Roles of active site residues and the HUH motif of the F plasmid TraI relaxase. J. Biol. Chem. **282:**33707–33713. http://dx.doi.org/10.1074/jbc.M703210200.
46. **Matson SW, Nelson WC, Morton BS.** 1993. Characterization of the reaction product of the oriT nicking reaction catalyzed by Escherichia coli DNA helicase I. J. Bacteriol. **175:**2599–2606.
47. **González-Pérez B, Carballeira JD, Moncalian G, de la Cruz F.** 2009. Changing the recognition site of a conjugative relaxase by rational design. Biotechnol. J. **4:**554–557. http://dx.doi.org/10.1002/biot.200800184.
48. **Dostál L, Schildbach JF.** 2010. Single-stranded DNA binding by F TraI relaxase and helicase domains is coordinating regulated. J. Bacteriol. **192:**3620–3628. http://dx.doi.org/10.1128/JB.00154-10.
49. **Edwards JS, Betts L, Frazier ML, Pollet RM, Kwong SM, Walton WG, Ballentine WK, Huang JJ, Habibi S, Del Campo M, Meier JL, Dervan PB, Firth N, Redinbo MR.** 2013. Molecular basis of antibiotic multiresistance transfer in Staphylococcus aureus. Proc. Natl. Acad. Sci. U. S. A. **110:**2804–2809. http://dx.doi.org/10.1073/pnas.1219701110.
50. **Paterson ES, More MI, Pillay G, Cellini C, Woodgate R, Walker GC, Iyer VN, Winans SC.** 1999. Genetic analysis of the mobilization and leading regions of the IncN plasmids pKM101 and pCU1. J. Bacteriol. **181:**2572–2583.
51. **Paterson ES, Iyer VN.** 1992. The oriT region of the conjugative transfer system of plasmid pCU1 and specificity between it and the *mob* region of other N *tra* plasmids. J. Bacteriol. **174:**499–507.
52. **Paterson ES, Iyer VN.** 1997. Localization of the *nic* site of IncN conjugative plasmid pCU1 through formation of a hybrid *oriT*. J. Bacteriol. **179:**5768–5776.
53. **Nash RP, Habibi S, Cheng Y, Lujan SA, Redinbo MR.** 2010. The mechanism and control of DNA transfer by the conjugative relaxase of resistance plasmid pCU1. Nucleic Acids Res. **38:**5929–5943. http://dx.doi.org/10.1093/nar/gkq303.
54. **Nash RP, Niblock FC, Redinbo MR.** 2011. Tyrosine partners coordinate DNA nicking by the Salmonella typhimurium plasmid pCU1 relaxase enzyme. FEBS Lett. **585:**1216–1222. http://dx.doi.org/10.1016/j.febslet.2011.03.043.
55. **Kiianitsa K, Solinger JA, Heyer W-D.** 2003. NADH-coupled microplate photometric assay for kinetic studies of ATP-hydrolyzed enzymes with low and high specific activities. Anal. Biochem. **321:**266–271. http://dx.doi.org/10.1016/S0003-2697(03)00461-5.
56. **Grohmann E, Muth G, Espinosa M.** 2003. Conjugative plasmid transfer in Gram-positive bacteria. Microbiol. Mol. Biol. Rev. **67:**277–301. http://dx.doi.org/10.1128/MMBR.67.2.277-301.2003.
57. **Stern JC, Schildbach JF.** 2001. DNA recognition by F factor TraI36: highly sequence-specific binding of single-stranded DNA. Biochemistry **40:**11586–11595. http://dx.doi.org/10.1021/bi010877q.
58. **Jenkins WT.** 1991. The pyruvate kinase-coupled assay for ATPases: a critical analysis. Anal. Biochem. **194:**136–139. http://dx.doi.org/10.1016/0003-2697(91)90160-U.
59. **González-Pérez B, Carballeira JD, Moncalián G, de la Cruz F.** 2009. Changing the recognition site of a conjugative relaxase by rational design. Biotechnol. J. **4:**554–557. http://dx.doi.org/10.1002/biot.200800184.
60. **Abdel-Monem M, Hoffmann-Berling H.** 1976. Enzymic unwinding of DNA. 1. Purification and characterization of a DNA-dependent ATPase from Escherichia coli. Eur. J. Biochem. **65:**431–440.
61. **Kelley LA, Sternberg MJE.** 2009. Protein structure prediction on the Web: a case study using the Phyre server. Nat. Protoc. **4:**363–371. http://dx.doi.org/10.1038/nprot.2009.2.
62. **Guogas LM, Kennedy SA, Lee J-H, Redinbo MR.** 2009. A novel fold in the TraI relaxase-helicase C-terminal domain is essential for conjugative DNA transfer. J. Mol. Biol. **386:**554–568. http://dx.doi.org/10.1016/j.jmb.2008.12.057.